Available online at www.sciencedirect.com

SciVerse ScienceDirect

Journal of the European Ceramic Society 32 (2012) 2325–2331

www.elsevier.com/locate/jeurceramsoc

Synthesis of $La_{0.9}Sr_{0.1}Ga_{0.8}Mg_{0.2}O_{2.85}$ powder by gel combustion route with two-step doping strategy

Alberto Lapina[a], Shuai Li[a,b], Bill Bergman[a], Zhe Zhao[a,b,*]

[a] KTH Royal Institute of Technology, Department of Materials Science and Engineering, Division of Ceramic Technology, SE-10044 Stockholm, Sweden
[b] Stockholm University, Department of Materials and Environmental Chemistry, Arrhenius Laboratory, SE-10691 Stockholm, Sweden

Received 25 August 2011; received in revised form 24 January 2012; accepted 25 January 2012

Abstract

A two-step doping strategy was applied to the synthesis of $La_{0.9}Sr_{0.1}Ga_{0.8}Mg_{0.2}O_{2.85}$ (LSGM1020) powder by a gel combustion method. The Mg-doped $LaGaO_3$ powder was prepared in the first step, and Sr incorporation in the Mg-doped $LaGaO_3$ powder was done in the second step to obtain the final LSGM1020 powder. The two-step procedure is effective in preparing higher purity powders than the traditional one-step procedure. Rietveld refinement of X-ray powder diffraction (XRD) patterns shows that incorporation of Mg in $LaGaO_3$ in the first step enlarges the $LaGaO_3$ lattice: this facilitates the incorporation of Sr in the second doping step and thus high purity powder is obtained. Relatively phase pure LSGM1020 powder with only 3.1% of $LaSrGaO_4$ was obtained after calcination at 1300 °C for 5 h. Therefore, the two-step doping strategy is an effective procedure for the preparation of LSGM powders with high Sr- and Mg-doping levels.

Keywords: Lanthanum gallate; Perovskite; X-ray methods; Powders-chemical preparation; Sol–gel processes

1. Introduction

The perovskite lanthanum gallate doped with strontium and magnesium (LSGM) is a promising electrolyte material for intermediate temperature solid oxide fuel cells (SOFCs). It exhibits ionic conductivity higher than 0.10 S/cm at 800 °C and no electronic conduction is detected in the oxygen partial pressure range 10^{-20} atm $< P_{O_2} <$ 1 atm.[1,2] High Sr and Mg contents increase the oxygen vacancy concentration and thus the ionic conductivity,[3] but concentrations of dopants must stay within the solubility limits to avoid secondary phases.[4] It has been reported that the conductivity of LSGM electrolyte reaches a maximum and then decreases with increasing concentration of dopants.[5,6] To the best of our knowledge, the highest conductivity reported so far is 0.17 S/cm at 800 °C for pure-phase $La_{0.8}Sr_{0.2}Ga_{0.83}Mg_{0.17}O_{3-\delta}$.[5]

To obtain highly conductive LSGM electrolyte, phase pure LSGM powders having desired Sr and Mg concentrations are necessary.[2] Secondary phases such as $La_4Ga_2O_9$, $LaSrGa_3O_7$, and $LaSrGaO_4$ exhibit low conductivities. Their presence in LSGM depletes the perovskite phase of Ga and La, inducing cation vacancies and reducing oxygen ion conductivity.[4]

Moreover, high density and controlled microstructural morphology are necessary to have high ionic conductivity in the final ceramic material. Lower relative density of the electrolyte results in higher grain boundary resistance. A linear correlation between grain boundary conductivity and porosity for YSZ was reported by Gibson et al.[7] Liu et al.[8] reported that LSGM conductivity increases with increasing relative density, because of a decrease in amount of the cavities. Furthermore, agglomeration-free powders with the appropriate morphology are crucial to get an electrolyte with high ionic conductivity.[9] For instance, the conductivity of Sm-doped CeO_2 depends on particle morphology: sintering spherical particles instead of elongated particles produces a ceramic material with higher conductivity.

The solid state reaction (SSR) synthesis technique has been used for decades to prepare ceramic powders, but the chemical homogeneity of the as-prepared LSGM is often not satisfying and high sintering temperatures are needed.

---

* Corresponding author at: KTH Royal Institute of Technology, Department of Materials Science and Engineering, Division of Ceramic Technology, SE-10044 Stockholm, Sweden. Tel.: +46 87908324.
E-mail address: zhezhao@kth.se (Z. Zhao).

0955-2219/$ – see front matter © 2012 Published by Elsevier Ltd.
doi:10.1016/j.jeurceramsoc.2012.01.033

Table 1
Literature summary: LSGM electrolyte synthesis techniques.

Synthesis technique	Composition	Calcination/sintering	Phase purity	Powder morphology	Reference
Coprecipitation	$La_{0.8}Sr_{0.2}Ga_{0.83}Mg_{0.17}O_{2.815}$	1400 °C 4 h calcination	Pure phase	50 nm particles, agglomeration	10
Sol–gel	$La_{0.9}Sr_{0.1}Ga_{0.9}Mg_{0.1}O_{2.9}$ $La_{0.85}Sr_{0.15}Ga_{0.8}Mg_{0.2}O_{2.825}$ $La_{0.8}Sr_{0.2}Ga_{0.85}Mg_{0.15}O_{2.825}$	1500 °C 10 h sintering	Almost phase pure with MgO segregation		11
Sol–gel	$La_{0.8}Sr_{0.2}Ga_{0.8}Mg_{0.2}O_{2.8}$	1475 °C 20 h sintering	>99%		12
Pechini	$La_{0.8}Sr_{0.2}Ga_{0.83}Mg_{0.17}O_{2.815}$	1400 °C 6 h sintering	Pure phase	150 nm particles	10
Pechini	$La_{0.8}Sr_{0.2}Ga_{0.85}Mg_{0.15}O_{2.825}$ $La_{0.9}Sr_{0.1}Ga_{0.9}Mg_{0.1}O_{2.9}$ $La_{0.85}Sr_{0.15}Ga_{0.85}Mg_{0.15}O_{2.85}$	1400 °C 9 h calcination	Almost phase pure with MgO segregation		11
Pechini	$La_{0.8}Sr_{0.2}Ga_{0.83}Mg_{0.17}O_{2.815}$	1400 °C 8 h calcination	4–5% $LaSrGa_3O_7$, $LaSrGaO_4$		13
Pechini, with microwave heating	$La_{0.8}Sr_{0.2}Ga_{0.83}Mg_{0.17}O_{2.815}$	1400 °C 9 h calcination	6.2% $LaSrGaO_4$		14
Pechini, with microwave heating	$La_{0.8}Sr_{0.2}Ga_{0.85}Mg_{0.15}O_{2.825}$	1400 °C 8 h sintering	Pure phase		15
Acrylamide polymerization	$La_{0.9}Sr_{0.1}Ga_{0.8}Mg_{0.2}O_{2.85}$	1300 °C 5 h calcination	Small amounts of $LaSrGaO_4$, $Sr_3Ga_2O_6$		17
Acrylamide polymerization	$La_{0.85}Sr_{0.15}Ga_{0.85}Mg_{0.15}O_{2.85}$	1500 °C 15 h sintering	Small amount of $LaSrGa_3O_7$	Flat-like powder agglomerates	18
Gel combustion	$La_{0.85}Sr_{0.15}Ga_{0.9}Mg_{0.1}O_{2.85}$	1450 °C 5 h sintering	Pure phase		19
Gel combustion	$La_{0.8}Sr_{0.2}Ga_{0.83}Mg_{0.17}O_{2.815}$	1400 °C 9 h calcination	7% of $LaSrGaO_4$, $LaSrGa_3O_7$		20

Homogeneous distribution of the different cations in the powders prior to calcination is crucial, and chemical routes seem to be promising with respect to this. Different chemical routes have been used to synthesize LSGM, for example coprecipitation,[10] sol–gel method,[11,12] Pechini method,[10,12–16] acrylamide polymerization method[17,18] and gel combustion method.[19,20] A summary of the published results is reported in Table 1. Firstly, it can be found that calcination or sintering temperatures higher than 1400 °C are used to get high purity powders of different compositions with various synthesis techniques. There are reports that even a heat-treatment at 1500 °C is not enough to reach phase purity.[11,12] Secondly, phase pure powders can hardly be prepared with present methods. Although Huang and Goodenough[10] reported the successful preparation of pure phase $La_{0.8}Sr_{0.2}Ga_{0.83}Mg_{0.17}O_{2.815}$ by coprecipitation or Pechini method, powders with other compositions are rarely reported to be produced phase pure. Moreover, improvement of the synthesis method may prepare better powders. For instance, Zhai et al.[14] introduced microwave heating in the traditional Pechini method. The microwave heating apparently improves phase purity, but the $La_{0.8}Sr_{0.2}Ga_{0.83}Mg_{0.17}O_{2.815}$ powder calcined at 1400 °C still contains 6.2 wt% of secondary phases. In conclusion, further improvements of the synthesis techniques are required to guarantee preparation of phase pure material while lowering the heat treatment temperatures.

In this work we present a new synthesis procedure for LSGM, based on the division of the doping process into two steps. Mg and Sr were added in separate stages of the synthesis procedure, while usually all dopants are added at the same time. The addition of Mg to $LaGaO_3$ enlarges the unit cell,[21–24] and this may facilitate the accommodation of Sr in the lanthanum lattice in the second step of doping process. Furthermore, less secondary phases should be formed with fewer elements involved in each step.[13,21] The LSGM1020 ($La_{0.9}Sr_{0.1}Ga_{0.8}Mg_{0.2}O_{2.85}$) powder was prepared by a gel combustion method[25–27] using PAM (polyacrylamide) as polymer carrier. The choice of the carrier is due to its low decomposition temperature,[28] which eases the removal during calcination.

2. Experimental

The following chemicals were used to synthesize the powders: Ga_2O_3 (99.999%), $La_2(CO_3)_3$, $SrCO_3$ (99.99%), MgO (99.95%), $Sr(NO_3)_2$ and polyacrylamide (PAM, $-CH_2CHCONH_2-$). The LSGM powders were synthesized using two different procedures, which we refer to as one-step and two-step procedure. The flow charts of these two procedures are shown in Figs. 1 and 2.

In the one-step procedure, Ga_2O_3, $La_2(CO_3)_3$, $SrCO_3$ and MgO were dissolved together in nitric acid aqueous solution at about 100 °C, and then a PAM solution was added. The PAM solution was prepared by dissolving an appropriate amount of polyacrylamide in distilled water at room temperature. The amount of PAM was calculated according to an established ratio of positively charged valences to PAM monomers (M^{n+}/PAM) of 2:1. The precursor solution obtained was stirred and homogenized on a hot plate at room temperature for 2 h. Then it was

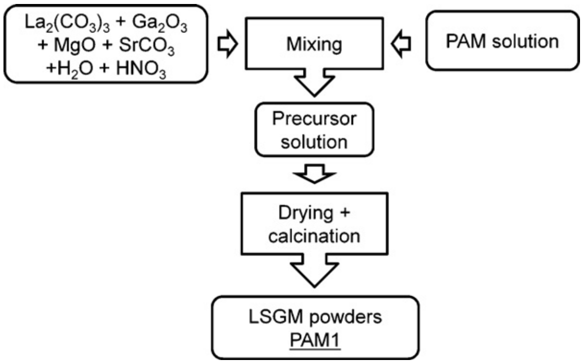

Fig. 1. Flow chart of the one-step synthesis procedure.

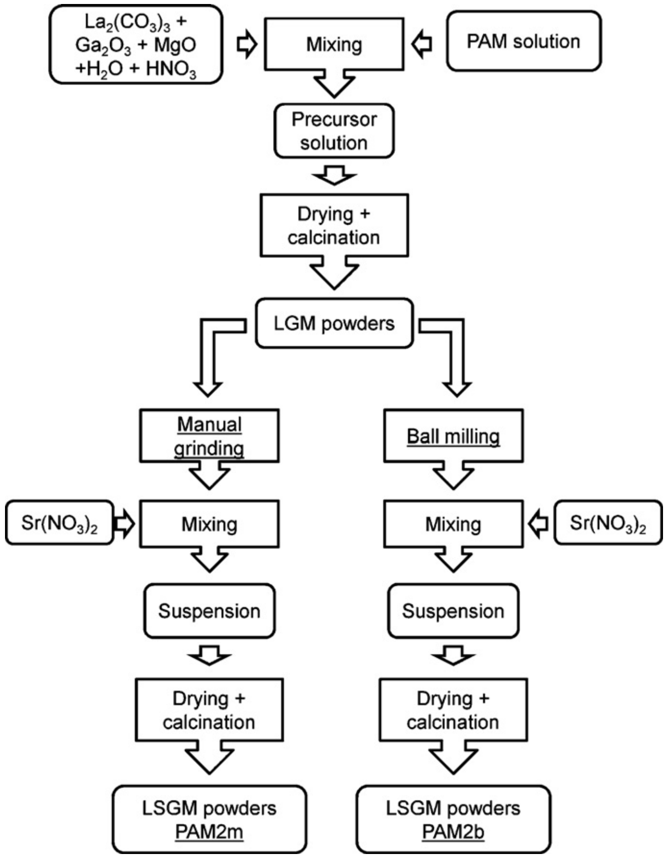

Fig. 2. Flow chart of the two-step synthesis procedure.

heated up to 130 °C while stirring to evaporate water and finally placed in an oven at 130 °C to dry completely. The gel obtained was grinded into fine powders and calcined in air at 800 °C for 10 h. The LSGM powders prepared by the one-step procedure are referred to as PAM1.

The two-step procedure consisted in splitting the doping process into two parts. In the first step, the same procedure as for the one-step procedure was followed, but $SrCO_3$ was not added. The LGM (magnesium-doped lanthanum gallate) powders produced after the first step were grinded either manually in a mortar or by ball milling. Planetary ball milling was performed using ZrO_2 balls as milling media and isopropyl alcohol as solvent. In the second step, the LGM powders were mixed with a stoichiometric amount of $Sr(NO_3)_2$ in distilled water at room temperature: the suspension was stirred to reach homogeneity. A small amount of PAM was added as dispersing agent to prevent agglomeration and the suspension was dried at 130 °C on a hot plate. The manually grinded powder is referred to as PAM2m, and the ball milling treated powder is referred to as PAM2b. Both LSGM powders then underwent manual grinding and calcination for 10 h in the temperature range 800–1300 °C.

The phases in calcined powders were analyzed using powder X-ray diffraction (XRD) (X'Pert Pro, PANalytical). Scans were taken with Cu Kα1 radiation (45 kV, 40 mA). The relative amount of secondary phases was estimated by the ratio of the total integrated intensities of the most intense XRD peaks of secondary phases over the integrated intensity of the most intense peak of the perovskite phase.[11,12] Rietveld refinement of the collected data was made using the Fullprof program. The morphology of powders was studied by scanning electron microscope (SEM, JSM-7000F JEOL).

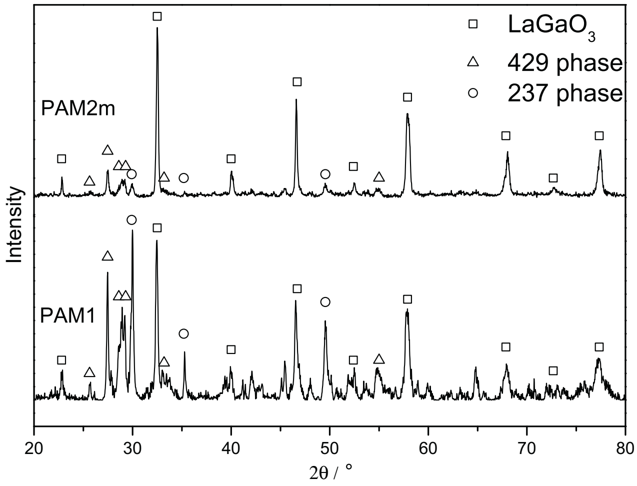

Fig. 3. XRD patterns for LSGM powders produced by one-step (PAM1, 43% $LaGaO_3$ phase) and two-step procedures (PAM2m, 85% $LaGaO_3$ phase) after calcination at 800 °C for 10 h.

3. Results and discussion

3.1. *Effect of two-step doping strategy*

Fig. 3 shows the XRD patterns of the calcined powders prepared by the two-step and the traditional one-step procedure respectively. Three different phases can be detected in the patterns: the perovskite $LaGaO_3$ phase (JCPDS 24-1102) and the secondary phases $La_4Ga_2O_9$ (429 phase, JCPDS 53-1108) and $LaSrGa_3O_7$ (237 phase, JCPDS 45-0637). While the PAM1 powder contains only 43% of $LaGaO_3$ phase, this value goes up to 85% in the PAM2m powder. The PAM2m powder thus consists of much more $LaGaO_3$ phase, showing that the two-step doping strategy can significantly promote the formation of perovskite $LaGaO_3$ phase in the calcined powder. Because of the different synthesis procedures, the two powders experience different heat treatment times (respectively 10 and 20 h). However the reaction-controlling diffusion kinetics are slow because of the low calcination temperature (800 °C), thus a difference in calcination time can be responsible only for small changes in phase composition of the powders. The large difference in phase purity between the two powders shows instead that the two-step procedure is more effective to prepare high purity LSGM powders than the traditional one-step procedure. In order to see the limit of the improvement in phase purity by two-step procedure, PAM2m powder was calcined also at higher temperatures. Fig. 4 shows the XRD patterns of the calcined PAM2m powders at various temperatures. All these powders are mainly characterized with perovskite $LaGaO_3$ phase, and the secondary phase $LaSrGaO_4$ (214 phase, JCPDS 24-1208) is also detected besides the 429 phase and 237 phase. Table 2 shows the fraction of the secondary phases in PAM2m powders

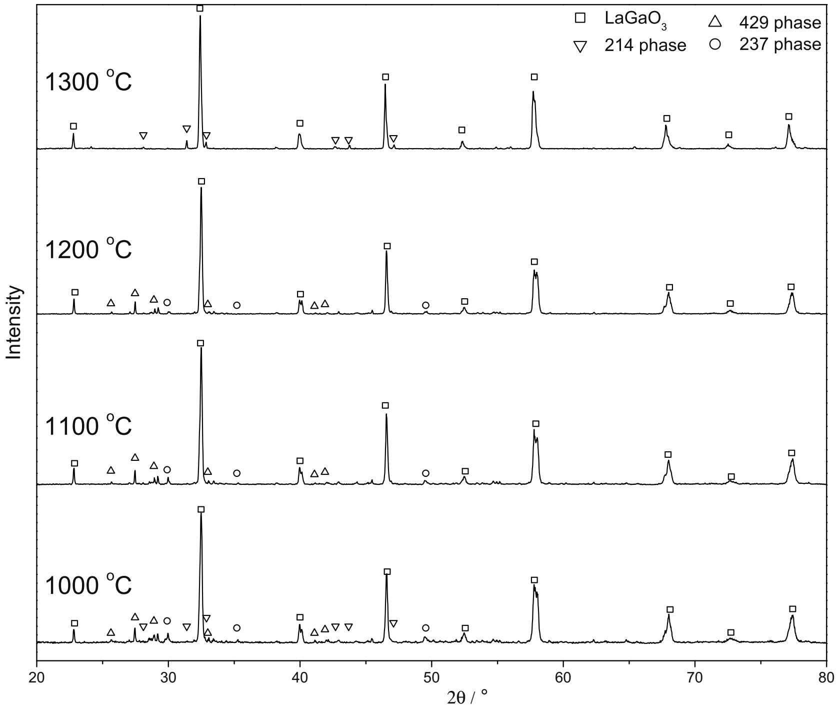

Fig. 4. XRD patterns for PAM2m powders produced with two-step procedure, after calcination for 10 h at (a) 1000 °C, (b) 1100 °C, (c) 1200 °C, and (d) 1300 °C.

calcined at various temperatures. The amount of 429 phase and 237 phase decrease continuously with increasing calcination temperature. However the 214 phase, which is almost absent after calcination at lower temperatures, increases to 3.1% after calcination at 1300 °C. Table 2 shows that the phase purity of LSGM powders increases together with the temperature of the final calcination, which is in good agreement with other works.[11,13,19] Rozumek et al.[29] report that for LSGM1020 in the temperature range 1100–1500 °C, the perovskite phase is in equilibrium with the secondary phases 214, 429 and MgO. Higher temperatures increase the solubility of Mg and Sr in the perovskite phase, thus explaining the reduction in content of secondary phases in our LSGM powder. MgO is not detected in our powder but could be present in amounts too small to be detected by XRD analysis. While the presence of MgO can be expected according to the phase diagrams mentioned previously, the presence of 237 secondary phase after calcination in the range 1000–1200 °C is not expected. It has however been reported by various authors that secondary phases depend on the synthesis method,[18,30] and this issue has not been clarified yet.

Table 2
Estimation of the amount of secondary phases in PAM2m powders.

Calcination temperature	$La_4Ga_2O_9$ (%) 429 phase	$LaSrGa_3O_7$ (%) 237 phase	$LaSrGaO_4$ (%) 214 phase	Total (%)
1000 °C	5.0	2.8	0.2	8.0
1100 °C	4.2	2.3	0.0	6.5
1200 °C	4.0	0.5	0.0	4.5
1300 °C	0.0	0.0	3.1	3.1

The phase purity of LSGM in this work after calcination at 1000 °C is similar to the one reported by Tas et al.[13] and Zhai et al.[14] using Pechini method and heat treatment at 1400 °C. Considering works using a gel combustion method, Li et al.[19] prepare $La_{0.85}Sr_{0.15}Ga_{0.85}Mg_{0.15}O_{2.85}$ powders using PVA (polyvinyl alcohol) as polymeric carrier, obtaining 11.3% of secondary phases after calcination at 1200 °C. Zhai et al.[20] improve this gel combustion method by introducing microwave heating and get a minimum 7% of secondary phases in $La_{0.8}Sr_{0.2}Ga_{0.83}Mg_{0.17}O_{2.815}$ calcined at 1400 °C. In the present work, the PAM2m powder calcined at 1300 °C contains only 3.1% of $LaSrGaO_4$, showing improvement in the LSGM powder phase purity at a lower temperature than the previously cited studies. Coprecipitation[10] and other sol–gel routes[17,18] require instead treatments at 1400 °C or 1500 °C to limit secondary phases content. These last works do not report numerical data about secondary phase content, thus a numerical comparison is not possible. It can be concluded that the two-step gel combustion method is an effective method for LSGM preparation.

3.2. Rietveld analysis for Mg^{2+} and Sr^{2+} incorporation in $LaGaO_3$ lattice

It is believed that the incorporation of Mg in the B site in the first step led to enlarged $LaGaO_3$ cell which may facilitate further insertion of Sr in the A site. To prove this, Rietveld pattern refinement of the XRD patterns was performed to resolve the cell parameters of the LGM calcined powder and LSGM calcined powder. In this work, the crystal structure which can give the best fit is orthorhombic, with space group of *Pbnm*.[24,31] The Rietveld refinement of the LGM is shown in Fig. 5. The 800 °C calcined LGM powder consists of 95% of $LaGaO_3$ phase, much more than

Table 3
Rietveld refinement results for the calcined powders of LGM and LSGM.

Specimen	*a* (Å)	*b* (Å)	*c* (Å)	Volume (Å^3)	[b]$\mathrm{Occ}_{\mathrm{La}}$	[b]$\mathrm{Occ}_{\mathrm{Sr}}$	[b]$\mathrm{Occ}_{\mathrm{Ga}}$	[b]$\mathrm{Occ}_{\mathrm{Mg}}$	Chi2
LGM	5.53594(0)	5.49783(0)	7.79210(0)	237.157	0.5	0	0.462(5)	0.038(5)	4.15
PAM2m	5.53519(0)	5.49982(0)	7.79453(0)	237.285	0.457(15)	0.043(15)	0.444(9)	0.056(9)	3.26
[a]$LaGaO_3$	5.52432(2)	5.49246(2)	7.77448(4)	235.89	0.5	0	0.5	0	

[a] ICSP database.
[b] Occ is the occupancy ratio of specified element in cation La and Ga sites of $LaGaO_3$ cell.

for the PAM1 powder. It is clear that the addition of Mg in the first step has the advantage of reducing the amount of undesired secondary phases. The refinement results of LGM powder are shown in Table 3. Occupancy ratio of Sr/Mg in Table 3 gives information of the dopant content of Sr/Mg in $LaGaO_3$ cell. The cell parameters of LGM powder are larger than those of the pure $LaGaO_3$ phase in Table 3, which illustrates the fact that Mg is successfully added into the $LaGaO_3$ cells. However, only 7.6% of the B sites are occupied by Mg atoms in the LGM powders, which is far less than the desired doping content of 20%. The extra Mg could remain in the powder in the form of MgO in amounts too small to be detected by XRD analysis. The incomplete dissolution of Mg in the $LaGaO_3$ lattice can be due to a dissolution limit of Mg in $LaGaO_3$[32,33] or to a heat treatment time too short to allow complete reaction.[13]

Fig. 6 shows the Rietveld refinement of the PAM2m XRD pattern. The cell parameters of this PAM2m powder show values similar to those of the LGM powder (Table 3). Mg doping in the first step provides enlarged cells which readily accommodate Sr addition in the second step. Although the ionic radius of Sr^{2+} is larger than that of La^{3+}, the cell parameters of PAM2m show decrease of *a*, and only small increment of *b* and *c*, as compared to those of LGM. This is due to the fact that introducing Sr into the lattice reduces the tilt of GaO_6 octahedra around *b* and *c* axes.[22,24] The already existing $LaGaO_3$ lattice, enlarged by Mg addition in the first step, provides a preferable accommodation for the incorporation of Sr in the second step, and thus facilitates the formation of LSGM perovskite. The relative amount of $LaGaO_3$ phase in the 1200 °C calcined PAM2m powder is 95.5%. 11.2% of the B sites are occupied by Mg, with only a small increase compared to LGM powder; 8.6% of the A sites are instead occupied by Sr. The remaining Sr is present in the form of 237 secondary phase, while the Mg not incorporated in the perovskite is probably present as MgO, but in amounts too small to be detected by XRD analysis. Because of this, the total

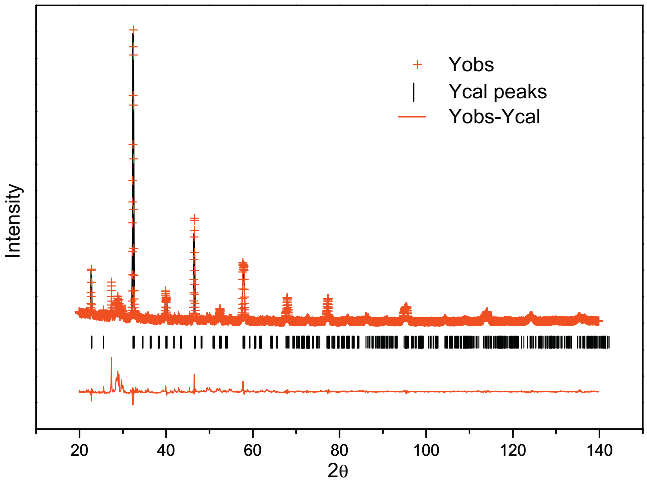

Fig. 5. Rietveld refinement of XRD of LGM calcined at 800 °C. The observed (Y_{obs}) pattern and the difference between the observed and calculated pattern ($Y_{obs} - Y_{cal}$) are plotted. Positions of the calculated peaks (Y_{cal} peaks) are indicated by vertical bars.

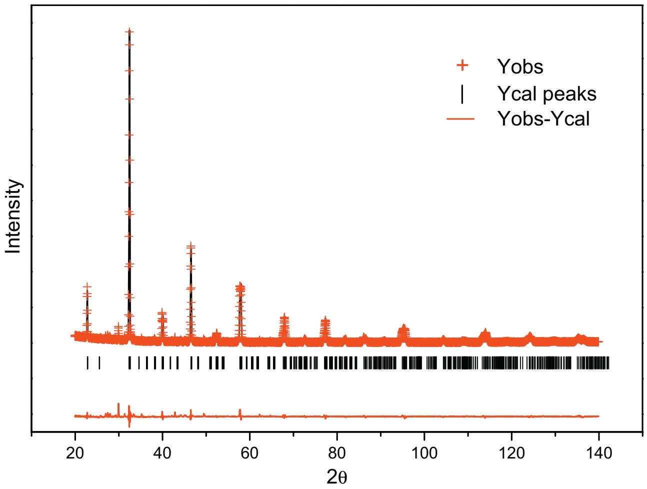

Fig. 6. Rietveld refinement of XRD of PAM2m calcined at 1200 °C 10 h. The observed (Y_{obs}) pattern and the difference between the observed and calculated pattern ($Y_{obs} - Y_{cal}$) are plotted. Positions of the calculated peaks (Y_{cal} peaks) are indicated by vertical bars.

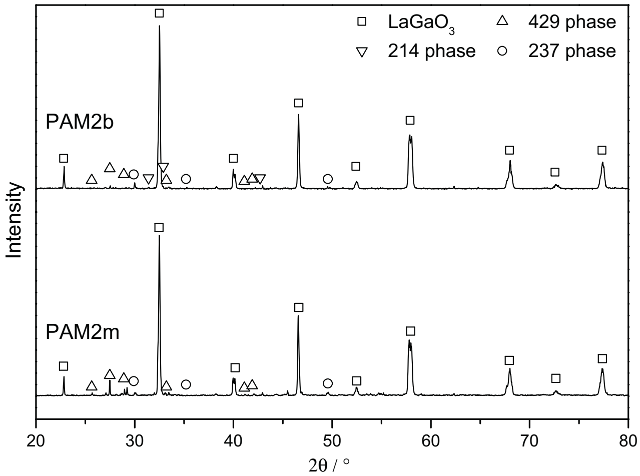

Fig. 7. XRD patterns of LSGM powders after calcination at 1200 °C for 10 h.

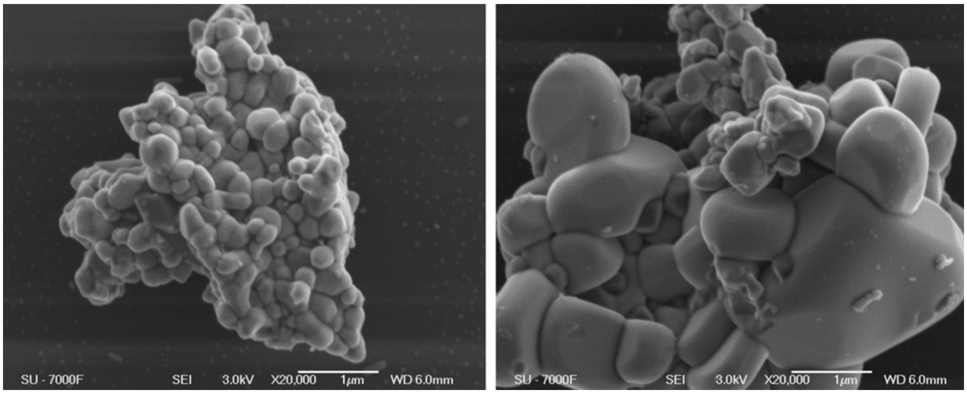

Fig. 8. SEM images of the powder morphology of PAM2b powder calcined at 1200 °C.

amount of secondary phases could be higher than what reported in Table 2.

3.3. Ball milling effect

The ball milling process on one hand can break up the agglomerates in the powders, and on the other hand facilitates phase formation by mechanical alloying.[17] In the present work, ball milling was introduced in the two-step procedure to prepare the powders: it was performed on LGM powders. In Fig. 7, XRD patterns show the influence of ball milling on the phases in the calcined LSGM powder. The amount of 429 secondary phase is reduced from 4% to 0.6% by ball milling, and the total amount of secondary phases changes from 4.5% in the PAM2m powder to 2.6% in the PAM2b powder. This means that ball milling is effective in reducing secondary phases in the calcined powder. So far, we have shown that the two-step procedure can successfully prepare fine LSGM powders with high phase purity. The preparation of a phase pure LSGM powder is of great importance for the phase purity and stoichiometry of the final sintered specimen, but as a matter of fact, the control of the powder morphology is also rather essential for the sintering properties. Fig. 8 shows the powder morphology of the PAM2b powder calcined at 1200 °C. It is found that small particles, ~150 nm in size, exist in the as-prepared powder; however big particles with micrometer size range are also found, suggesting a wide size distribution in the LSGM powders. Besides, the powder exhibits agglomeration. Fine and homogeneous powder morphology is expected to facilitate the final sintering process, and the morphology of powders is still not satisfactory at the present stage.

4. Conclusions

The LSGM powder was prepared using the gel combustion method with the introduction of the two-step doping strategy. First Mg was added to obtain the Mg-doped $LaGaO_3$, and then Sr was added in the second step to have the final LSGM powder. The two-step method is better than the traditional one-step procedure to prepare pure phase LSGM powders. The Mg addition in the first step forms the Mg doped $LaGaO_3$ phase, thus enlarging the $LaGaO_3$ lattice and facilitating the Sr doping in the second step. This is proved by the Rietveld full pattern refinement of the XRD patterns of LGM and LSGM powders. However, the Rietveld refinement results also show that only 8.6% of La sites and 11.2% of Ga sites are respectively occupied by Sr and Mg: these values are lower than expected. The LSGM powder obtained after calcination at 1300 °C for 10 h contains 3.1% of 214 secondary phase and probably also a small amount of MgO not detectable by XRD. The ball milling of LGM precursor powders is effective in further reducing the amount of secondary phases in the calcined LSGM powder. A high purity LSGM with 97.4% of $LaGaO_3$ perovskite was obtained after the ball milling process. This suggests that the two-step procedure with ball milling is effective in preparing phase pure LSGM powders. Concerning the morphology, the as-prepared LSGM powder contains hard agglomeration with seriously sintered particles and uneven particle sizes: powder morphology and sintering behavior will be presented in future work.

References

1. Ishihara T, Matsuda H, Takita H. Doped $LaGaO_3$ perovskite type oxide as a new oxide ionic conductor. *J Am Ceram Soc* 1994;**116**:3801–3.
2. Huang P, Petric A. Superior oxygen ion conductivity of lanthanum gallate doped with strontium and magnesium. *J Electrochem Soc* 1996;**143**:1644–8.
3. Singhal SC, Kendall K. *High temperature solid oxide fuel cells: fundamentals, design and application*. Elsevier; 2003.
4. Datta P. Doped $LaGaO_3$ based solid oxide fuel cell materials and their sintering. *Mater Sci Forum* 2009;**624**:109–37.
5. Huang K, Tichy RS, Goodenough JB. Superior perovskite oxide-ion conductor; strontium- and magnesium-doped $LaGaO_3$: I. Phase relationships and electrical properties. *J Am Ceram Soc* 1998;**81**:2565–75.
6. Li S, Bergman B. Doping effect on secondary phases, microstructure and electrical conductivities of $LaGaO_3$ based perovskites. *J Eur Ceram Soc* 2009;**29**:1139–46.
7. Gibson IR, Dransfield GP, Irvine JTS. Sinterability of commercial 8 mol% yttria-stabilised zirconia powders and the effect of sintered density on the ionic conductivity. *J Mater Sci* 1998;**33**:4297–305.
8. Liu N, Shi M, Wang C, Yuan YP, Majewski P, Aldinger F. Microstructure and ionic conductivity of Sr- and Mg-doped $LaGaO_3$. *J Mater Sci* 2006;**41**:4205–13.
9. Mori T, Wang Y, Drennan J, Auchterlonie G, Li J, Ikegami T. Influence of particle morphology on nanostructural feature and conducting property in Sm-doped CeO_2 sintered body. *Solid State Ionics* 2005;**175**:641–9.
10. Huang K, Goodenough JB. Wet chemical synthesis of Sr- and Mg doped $LaGaO_3$, a perovskite-type oxide-ion conductor. *J Solid State Chem* 1998;**136**:274–83.

11. Polini R, Pamio A, Traversa E. Effect of synthetic route on sintering behaviour, phase purity and conductivity of Sr- and Mg-doped $LaGaO_3$ perovskites. *J Eur Ceram Soc* 2004;**24**:1365–70.
12. Polini R, Falsetti A, Traversa E. Sol–gel synthesis and characterization of Co-doped LSGM perovskites. *J Eur Ceram Soc* 2005;**25**:2593–8.
13. Tas AC, Majewski PJ, Aldinger F. Chemical preparation of pure and strontium- and/or magnesium-doped lanthanum gallate powders. *J Am Ceram Soc* 2000;**83**:2954–60.
14. Zhai Y, Ye C, Xiao J, Dai L. A microwave-induced solution polymerization synthesis of doped $LaGaO_3$ powders. *J Power Sources* 2006;**163**:316–22.
15. Rambabu B, Ghosh S, Zhao W, Jena H. Innovative processing of dense LSGM electrolytes for IT-SOFC's. *J Power Sources* 2006;**159**:21–8.
16. Jena H, Rambabu B. An exploratory study on solution assisted synthetic routes to prepare nano-crystalline $La_{1-x}M_xGa_{1-y}N_yO_{3+[delta]}$ (M = Sr; N = Mn, Mg) for IT-SOFC applications. *Mater Chem Phys* 2007;**101**:20–9.
17. Tarancon A, Dezanneau G, Arbiol J, Peiro F, Morante JR. Synthesis of nanocrystalline materials for SOFC applications by acrylamide polymerization. *J Power Sources* 2003;**118**:256–64.
18. Liu N, Yupeng Y, Majewski P, Aldinger F. Synthesis of $La_{0.85}Sr_{0.15}Ga_{0.85}Mg_{0.15}O_{2.85}$ materials for SOFC applications by acrylamide polymerization. *Mater Res Bull* 2006;**41**:461–8.
19. Li Z, Zhang H, Bergman B, Zou X. Synthesis and characterization of $La_{0.85}Sr_{0.15}Ga_{0.85}Mg_{0.15}O_{3-[delta]}$ electrolyte by steric entrapment synthesis method. *J Eur Ceram Soc* 2006;**26**:2357–64.
20. Zhai Y, Ye C, Xia F, Xiao J, Dai L, Yang Y, et al. Preparation of $La_{0.8}Sr_{0.2}Ga_{0.83}Mg_{0.17}O_{2.815}$ powders by microwave induced poly(vinyl alcohol) solution polymerization. *J Power Sources* 2006;**162**:146–50.
21. Datta P, Majewski P, Aldinger F. Structural studies of Sr- and Mg-doped $LaGaO_3$. *J Alloys Compd* 2007;**438**:232–7.
22. Slater PR, Irvine JTS, Ishihara T, Takita Y. The structure of the oxide ion conductor $La_{0.9}Sr_{0.1}Ga_{0.8}Mg_{0.2}O_{2.85}$ by powder neutron diffraction. *Solid State Ionics* 1998;**107**:319–23.
23. Lerch M, Boysen H, Hansen T. High-temperature neutron scattering investigation of pure and doped lanthanum gallate. *J Phys Chem Solids* 2001;**62**:445–55.
24. Kajitani M, Matsuda M, Hoshikawa A, Oikawa K, Torii S, Kamiyama T, et al. Neutron diffraction study on lanthanum gallate perovskite compound series. *Chem Mater* 2003;**15**:3468–73.
25. Gulgun MA, Nguyen MH, Kriven WM. Polymerized organic–inorganic synthesis of mixed oxides. *J Am Ceram Soc* 1999;**82**:556–60.
26. Lee S, Benson EA, Kriven WM. Preparation of portland cement components by poly(vinyl alcohol) solution polymerization. *J Am Ceram Soc* 1999;**82**:2049–55.
27. Nguyen MH, Lee S, Kriven WM. Synthesis of oxide powders by way of a polymeric steric entrapment precursor route. *J Mater Res* 1999;**14**: 3417–26.
28. Smith EA, Prues SL, Oehme FW. Environmental degradation of polyacrylamides. 1. Effects of artificial environmental conditions: temperature, light, and pH. *Ecotox Environ Safe* 1996;**35**:121–35.
29. Rozumek M, Majewski P, Sauter L, Aldinger F. Homogeneity region of strontium- and magnesium-containing $LaGaO_3$ at temperatures between 1100 °C and 1500 °C in air. *J Am Ceram Soc* 2003;**86**: 1940–6.
30. Djurado E, Labeau M. Second phases in doped lanthanum gallate perovskites. *J Eur Ceram Soc* 1998;**18**:1397–404.
31. Rozumek M, Majewski P, Aldinger F. Metastable crystal structure of strontium- and magnesium-substituted $LaGaO_3$. *J Am Ceram Soc* 2004;**87**:656–61.
32. Gorelov VP, Bronin DI, Sokolova JV, Näfe H, Aldinger F. The effect of doping and processing conditions on properties of $La_{1-x}Sr_xGa_{1-y}Mg_yO_{3-[alpha]}$. *J Eur Ceram Soc* 2001;**21**:2311–7.
33. Matraszek A, Singheiser L, Kobertz D, Hilpert K, Miller M, Schulz O, et al. Phase diagram study in the La_2O_3–Ga_2O_3–MgO–SrO system in air. *Solid State Ionics* 2004;**166**:343–50.